

1 **Integrating planar polarity and tissue mechanics in computational models of**  
2 **epithelial morphogenesis**

3

4 Katherine H. Fisher<sup>1,2</sup>

5 David Strutt<sup>1,2</sup>

6 Alexander G. Fletcher<sup>1,3,\*</sup>

7

8 1 Bateson Centre, University of Sheffield, Firth Court, Western Bank, Sheffield, S10  
9 2TN

10 2 Department of Biomedical Science, University of Sheffield, Firth Court, Western  
11 Bank, Sheffield, S10 2TN

12 3 School of Mathematics and Statistics, University of Sheffield, Hicks Building,  
13 Hounsfield Road, Sheffield, S3 7RH

14

15 \* Corresponding author: [a.g.fletcher@sheffield.ac.uk](mailto:a.g.fletcher@sheffield.ac.uk)

16

17

18 **Abstract**

19

20 Cells in many epithelial tissues are polarised orthogonally to their apicobasal axis.  
21 Such planar polarity ensures that tissue shape and structure are properly organised.  
22 Disruption of planar polarity can result in developmental defects such as failed neural  
23 tube closure and cleft palate. Recent advances in molecular and live-imaging  
24 techniques have implicated both secreted morphogens and mechanical forces as  
25 orienting cues for planar polarisation. Components of planar polarity pathways act  
26 upstream of cytoskeletal effectors, which can alter cell mechanics in a polarised  
27 manner. The study of cell polarisation thus provides a system for dissecting the  
28 interplay between chemical and mechanical signals in development. Here, we  
29 discuss how different computational models have contributed to our understanding of  
30 the mechanisms underlying planar polarity in animal tissues, focusing on recent  
31 efforts to integrate cell signalling and tissue mechanics. We conclude by discussing  
32 ways in which computational models could be improved to further our understanding  
33 of how planar polarity and tissue mechanics are coordinated during development.

## 34 Introduction

35

36 A central problem in developmental biology is to understand how tissues form and  
37 repair in a highly reproducible manner. Key signalling molecules are spatially  
38 coordinated to provide positional information in developing tissues. While it has long  
39 been known that cells can sense and interpret such chemical gradients during  
40 pattern formation [1], mechanical forces are now recognised to also play a vital role  
41 in shaping tissues [2,3]. Increasing evidence suggests that these chemical and  
42 physical mechanisms are interconnected [4].

43

44 Morphogenesis is frequently driven by the dynamics of epithelial tissues, which line  
45 the majority of organs in the body. As well as being characterised by polarity along  
46 an apicobasal axis, epithelia often exhibit planar polarity orthogonally through the  
47 plane of the tissue (**Fig. 1A**) [5]. While it is possible for individual cells to become  
48 planar polarised, animal epithelial cells locally coordinate their polarity via  
49 intercellular transmembrane complexes (**Fig. 1B**) [6,7] to robustly generate uniform  
50 polarity across tissues, even when a global polarising signal is weak or noisy [8,9].

51

52 This coordinated polarity can be readily visualised by the formation of oriented  
53 external structures such as hairs or bristles (**Fig. 1B, C**). It is also vital for  
54 fundamental functional roles that require cell coordination, such as oriented division  
55 (**Fig. 1D**) and convergent extension (**Fig. 1E**), thus disruption of these mechanisms  
56 results in disease [10]. Research into planar polarity establishment focuses on how  
57 long-range morphogen and mechanical gradients are interpreted at the cellular level  
58 [11], how cells communicate to coordinate information from upstream cues [12], and  
59 how downstream effectors alter cell behaviour and the forces underlying tissue  
60 formation [13].

61

62 Given the complexity of these processes, computational modelling plays an  
63 increasingly useful role in aiding our mechanistic understanding [14]. A key challenge  
64 is to interface models that include descriptions of cell shape, mechanics, and  
65 signalling on different scales. In this review, we consider the contribution of  
66 computational modelling first to planar polarity establishment, then to downstream  
67 mechanics, and the novel computational methods that study the interplay between  
68 them. For brevity, we consider animal tissues only, focussing primarily on *Drosophila*  
69 since the majority of planar polarity components have been extensively studied in  
70 that system.

## 71 **Modelling planar polarity establishment**

72

73 Planar polarity can refer to any polarised protein or structure that breaks cellular  
74 symmetry in the plane of the tissue, occurring via multiple independent pathways.  
75 We begin by briefly summarising computational modelling of two key pathways: the  
76 Frizzled (Fz)-dependent or 'core' pathway, and the Fat (Ft)-Dachsous (Ds) pathway.  
77 We then describe the conserved anteroposterior (AP) patterning system active in the  
78 *Drosophila* embryonic epidermis.

79

### 80 *Core pathway*

81

82 Components of the core pathway form asymmetrically localised molecular bridges  
83 between cells. The transmembrane protein Flamingo (Fmi; Celsr in vertebrates) can  
84 homodimerise via its extracellular domain across *intercellular* junctions. Fmi interacts  
85 *intracellularly* with two other transmembrane proteins, Fz and Van Gogh (Vang),  
86 which recruit several cytoplasmic factors (**Fig. 2A**). Since Fmi can homodimerise, it  
87 exhibits axial asymmetry (enriched on both sides of cells), whereas all other factors  
88 exhibit vectorial asymmetry (enriched on one side) (**Fig. 1A**). Fz and Vang appear to  
89 be the key components for recruiting other factors to apical junctional domains [15]  
90 and mediating cell communication of polarity [16,17], whereas the cytoplasmic  
91 proteins are thought to be responsible for polarity establishment [18-20] by amplifying  
92 initial asymmetries in Fmi, Fz and Vang through feedback interactions. The outcome  
93 of this pathway dictates, for example, the orientation of hairs on the *Drosophila* wing  
94 surface (**Fig. 1B, C**).

95

96 A variety of mathematical models have been proposed for the molecular wiring  
97 underlying this amplification [21]. In these models, asymmetric complexes form at  
98 cell junctions and feedback interactions occur between complexed proteins, such  
99 that either 'like' complexes of the same orientation are stabilised, or 'unlike'  
100 complexes of opposite orientation are destabilised, generating bistability (**Fig. 2B**).  
101 These models vary in complexity and include those based on Turing pattern  
102 formation mechanisms, using deterministic [22,23] or stochastic [24] reaction-  
103 diffusion approaches, and others based on the Ising model of ferromagnetism, which  
104 treat each cell as a 'dipole' that locally coordinates its angle with its neighbours [25].  
105 Such models also vary in biological detail; from abstracted systems where two  
106 species bind to form a complex at junctions [26,27] to those including more defined  
107 molecular species. The latter necessitates many more kinetic parameters: for

108 example, the model by Amonlirdviman et al [22] contains nearly 40 rate constants,  
109 diffusion coefficients and conserved concentrations whose values had to be  
110 estimated.

111

112 Domineering non-autonomous phenotypes, where a clone of cells mutant for a  
113 polarity protein influences the polarity of wild-type neighbours (**Fig. 2C**), have formed  
114 the basis for validating core pathway models at the tissue scale. Whether considering  
115 a one-dimensional row of two-sided cells [27], or a two-dimensional field of  
116 hexagonal [22] or irregularly shaped cells [28], various models are able to  
117 recapitulate these phenotypes. Importantly, modelling has bolstered our intuition on  
118 how polarity may be established and highlighted critical conceptual factors necessary  
119 for the system to work. For example, both the Amonlirdviman [22] and Le Garrec [24]  
120 models can generate tissue-level planar polarity when provided with a transient,  
121 rather than sustained, polarity cue; however, transient cues are not sufficient to  
122 ensure robustness of the resulting cellular polarisation (**Fig. 2D**) [23]. A number of  
123 biological candidates for a persistent global bias have been suggested, including the  
124 directional trafficking of Fz complexes along microtubules [29,30].

125

#### 126 *Ft-Ds pathway*

127

128 In contrast to the core pathway, there is strong evidence for a primary role of  
129 morphogen gradients in orienting the Ft-Ds pathway. In developing tissues, upstream  
130 morphogens specify opposing tissue gradients of Four-jointed (Fj), a Golgi-tethered  
131 kinase and Ds, a cadherin [31]. Ft and Ds are single-pass transmembrane proteins  
132 that can heterodimerise across intercellular cell junctions (**Fig. 3A**). They are both  
133 phosphorylated by Fj, which alters their ability to bind to one another [32,33].

134 Interestingly, although similar domains are modified on each protein, phosphorylation  
135 of Ft appears to improve its ability to bind to Ds, while phosphorylation of Ds is  
136 inhibitory. Work in *Drosophila* shows that Ft and Ds become asymmetrically localised  
137 within cells and that in turn recruits the atypical myosin Dachs to the distal side of  
138 cells [33-35]. Polarisation of this pathway can regulate tissue growth via the Hippo  
139 signalling pathway [36] and tissue shape by modulating tension at cell-cell junctions  
140 and orienting cell divisions [34,37,38], as well as coupling to the core pathway via the  
141 Pk isoform, Spiny-legs (Sple) [39].

142

143 While abstracted planar polarity models [8,26,27] could in principle be applied to the  
144 Ft-Ds system, models tailored to specific molecular interactions are limited. A recent

145 phenomenological model examined the collective polarisation of the predominant  
146 complex – phosphorylated Ft ( $Ft^P$ ) binding unphosphorylated Ds ( $Ds^U$ ) – between  
147 cells in the *Drosophila* wing [40]. Either stabilising or destabilising feedback was  
148 found to amplify shallow graded inputs, but a combination of both more readily  
149 recapitulated experimental observations. By linking the strength of polarisation to a  
150 downstream tissue growth parameter, predictions were made and tested about the  
151 relationship between protein levels and overall tissue size.

152

153 Elsewhere, further molecular detail was included in a system of coupled ordinary  
154 differential equations describing interactions, again forming the predominant complex  
155 ( $Ft^P$  binding  $Ds^U$ ), in a one-dimensional row of cells [41]. However, for the majority of  
156 this study, the authors did not consider the orientation of those complexes at  
157 individual junctions, but only the asymmetry of total complexes across each cell, thus  
158 questions related to Ft and Ds polarity were not addressed. A more recent study  
159 used the *Drosophila* larval wing disc (**Fig. 3B**) to quantify the Fj gradient and Ds  
160 levels to initialise a one-dimensional reaction-diffusion model (**Fig. 3C**) [42]. Including  
161 all possible complexes of phosphorylated and unphosphorylated forms of Ft and Ds  
162 led to more uniform cellular polarity across the tissue (**Fig. 3D**). However, only  
163 considering the most favoured complex, as in previous models, resulted in greater  
164 variation in polarity and binding levels across the tissue. Coupled with experimental  
165 evidence, this supports the hypothesis that Fj acts on both Ft and Ds *in vivo*, but with  
166 opposing consequences, and illustrates the power of combining experimental and  
167 theoretical approaches in the same work.

168

### 169 *AP patterning system*

170

171 In the *Drosophila* embryo, elongation of the body axis, known as germ-band  
172 extension, is driven by polarised cell movements and appears to occur independently  
173 of the core and Ft-Ds pathways [43]. Instead, evidence suggests that it is guided by  
174 striped pair-rule gene expression [44,45], although some contribution is also afforded  
175 to oriented cell divisions [46] and large-scale mechanical deformations [47]. The  
176 complex upstream gene-regulatory network consists of maternally derived  
177 morphogen gradients patterning gap gene expression, leading to stripes of pair-rule  
178 gene expression [48]. While the gap gene network has been extensively studied  
179 theoretically, uncovering shifting expression boundaries and the importance of  
180 transient dynamics of gene regulation [49,50], modelling of striped pair-rule gene  
181 expression and downstream processes remains limited.

## 182 **Modelling planar polarity pathway regulation of cell mechanics**

183

184 The importance of mechanics in epithelial morphogenesis is well established [51].  
185 Furthermore, increasing evidence suggests that a common role of planar polarity  
186 pathways is the spatial patterning of cell mechanics to affect consequent tissue-level  
187 morphogenetic processes such as convergent extension. Studies in both *Drosophila*  
188 and vertebrates reveal that downstream effectors include regulators of myosin II,  
189 actin and cadherins [52,53], which in turn affect anisotropy of local forces within an  
190 epithelial tissue (**Fig. 4A**). For example, the core planar polarity pathway has been  
191 implicated in polarised modulation of cell adhesion through trafficking of the  
192 adherens junction molecule E-cadherin. This appears to influence cell packing in the  
193 *Drosophila* wing and cell intercalation in the trachea [54,55].

194

195 Nevertheless, models of polarity establishment typically assume that the dynamics of  
196 protein localisation occurs on a much faster timescale than cell shape changes, and  
197 thus consider a static cell packing geometry. To study dynamic cell shape changes  
198 requires coupling of models of planar polarity with tissue mechanics. To this end a  
199 variety of ‘cell-based’ models have been developed, which allow for the incorporation  
200 of cell signalling and feedback [56]. These include vertex [57] and cellular Potts [58]  
201 models, which approximate each cell’s apical surface by a polygon whose vertices  
202 move according to a force balance equation, or a set of pixels that change  
203 stochastically to minimize an energy function, respectively (**Fig. 4B**). Each approach  
204 has its strengths and limitations [59]. Here we discuss a number of example studies.

205

### 206 *Core pathway*

207

208 Inspired by evidence that the core planar polarity pathway can modulate cell  
209 mechanics, Salbreux et al [60] applied a vertex model to the ordered packing of cells  
210 in the zebrafish retina. Using a phenomenological differential equation model of  
211 planar polarity protein dynamics, the authors assumed that protein localisation  
212 modulates the ‘surface tension’ associated with cell-cell junctions and – through force  
213 balance – cell and tissue geometry. Geometry then feeds back on the localisation of  
214 planar polarity proteins. By comparing simulations under different hypotheses, the  
215 authors deduced that an extrinsic force (intraocular pressure) and progressive cell  
216 growth and division were required for the observed packing behaviour. Importantly,  
217 the authors tested model predictions by experiments with mutant fish such as those

218 exhibiting increased intraocular pressure. Such work exemplifies the power of an  
219 approach in which experiments and computational models are tightly integrated.

220

#### 221 *Ft-Ds pathway*

222

223 As discussed above, the *Drosophila* Ft-Ds pathway is required for the planar  
224 polarisation of the atypical myosin Dachs. This in turn is required for orienting cell  
225 divisions during morphogenesis [37]. More recently a direct correlation between  
226 Dachs polarisation, membrane tension and tissue shape during growth has been  
227 made using a combination of modelling and mutant clone experiments in the  
228 *Drosophila* pupal dorsal thorax [38]. Following from earlier work linking Ft-Ds to  
229 mechanical control of morphogenesis [34], the authors explored why Ft or Ds mutant  
230 clones are rounded in shape, appearing to minimise their contacts with neighbouring  
231 cells, a process which is dependent on Dachs [37]. Notably, Dachs is enriched at  
232 clone boundary junctions and reduced at transversal junctions, those perpendicular  
233 to the clone boundary within the clone (**Fig. 4C**). This polarisation of Dachs  
234 correlated with altered line tension of these junctions. A cellular Potts model, with  
235 differences in tension at particular interfaces, was able to accurately recapitulate the  
236 clone circularity observed *in vivo*.

237

#### 238 *AP patterning pathway*

239

240 In the *Drosophila* embryo, the aforementioned pair-rule gene expression stripes lead  
241 to enrichment of Myosin II at AP borders and the adapter protein Bazooka/Par3 at  
242 dorsoventral (DV) borders [45,61], the latter recruiting E-cadherin to form adherens  
243 junctions. Planar polarisation of Myosin II, which drives the selective shortening of  
244 cell-cell junctions during active cell intercalation in germ-band extension [61], was  
245 recently discovered to be mediated by overlapping expression domains of Toll-like  
246 receptors [62]. This provides a combinatorial code where every cell along the AP axis  
247 has a different 'identity'. To investigate how order is maintained as cells intercalate,  
248 Tetley et al [63] combined tissue-scale *in vivo* imaging and analysis with a vertex  
249 model incorporating differential junctional line tension between cells of different  
250 identities. Boundaries defined by polarised Myosin II, including parasegmental  
251 boundaries [47], were found to drive axis extension while at the same time limiting  
252 cell mixing. This work highlights the burgeoning recognition of the importance of  
253 'cables' and other planar enrichments of actomyosin in coordinating morphogenetic  
254 processes. Future modelling efforts should include more mechanically explicit

255 descriptions of how levels and polarisation of Myosin II and other effector proteins  
256 modulate cell mechanical properties. A pioneering example of such integration was  
257 recently proposed by Lan et al, who coupled modelling of polarisation of Rho-kinase,  
258 myosin and Bazooka with a vertex model, but restrict their attention to a relatively  
259 small number of cells [64].

260

261

## 262 **Interplay between mechanics and planar polarity**

263

264 The above work seeks to understand the geometric and mechanical consequences  
265 of planar polarity signalling at the tissue level. However, recent evidence points to  
266 there being feedback, with adhesion and tension affecting tissue patterning pathways  
267 [13]. An extensive study used time-lapse imaging of *Drosophila* pupal wing  
268 development over several hours coupled with a vertex model showing that external  
269 tension elongates cells along the proximodistal axis and dictates the orientation of  
270 planar polarity [65]. Similarly, in the developing *Xenopus* embryo, mechanical strain  
271 has been shown to orient the global polarity axis [66]. Furthermore, in the mouse  
272 skin, Celsr1 symmetry appears to be broken by mechanical deformation along one  
273 axis [67]. Together, these results suggest a general mechanism where planar polarity  
274 proteins perdure on persistent junctions and are slow to accumulate on newly formed  
275 junctions allowing oriented cell rearrangements and tissue deformations to induce a  
276 new axis of asymmetry [11]. This further suggests that in some contexts core planar  
277 polarity polarisation is a passive process, governed by tissue-level changes.  
278 Conversely, the *Drosophila* Ft-Ds pathway is able to resist tissue strain and maintain  
279 its polarity in response to the graded signal of Fj, suggesting it is actively remodelled  
280 [39]. This is an intriguing area for future study where computational modelling may  
281 help to unravel why these pathways behave differently.

282

283

## 284 **Concluding remarks**

285

286 We conclude by highlighting some extensions required to increase the utility of  
287 computational models in understanding planar polarity and tissue mechanics during  
288 development.

289

290 Several sources of biological complexity have not yet been incorporated or  
291 investigated within these models. A key consideration is the timescale over which a



292 tissue can establish or remodel the asymmetric distribution of planar polarity  
293 components within a cell, versus the timescale over which mechanical changes  
294 occur. Notably, the rate of planar polarisation is likely to be strongly influenced by  
295 mechanisms such as directed vesicular transport and recycling of planar polarity  
296 components, but these have so far been neglected in current models. Furthermore,  
297 the significance of stochasticity and variability in polarity protein interactions and  
298 signal interpretation remain to be addressed, even though *in vivo* these are likely to  
299 contribute a significant degree of noise.

300

301 While two-dimensional computational models of patterned epithelial have established  
302 themselves as important tools, three-dimensional models remain limited and are  
303 typically restricted to imposed, static anisotropies in mechanical properties [68]. The  
304 extension of such models to allow for the dynamic simulation of planar polarity  
305 signalling remains to be tackled. For example, an intriguing link between core  
306 pathway planar polarity and three-dimensional tissue deformations was found by  
307 Ossipova et al [69], who demonstrated that planar polarity-dependent polarisation of  
308 the recycling endosome marker Rab11 is required for apical constriction and  
309 subsequent epithelial folding in the *Xenopus* neural plate.

310

311 Several software tools have recently been released for automated cell segmentation,  
312 tracking, and shape and polarity quantification in epithelial tissues [70-72]. This has  
313 coincided with the development of techniques to measure, infer, and manipulate  
314 forces *in vivo* [73,74]. Ongoing technical challenges associated with integrating the  
315 resulting data within computational models include developing efficient methods of  
316 simulating, and performing parameter inference and uncertainty quantification, on  
317 such models. Addressing these challenges will help to place computational models of  
318 planar polarity and tissue mechanics on a more quantitative footing, advancing their  
319 biological realism and power to guide future experiments.

320

321

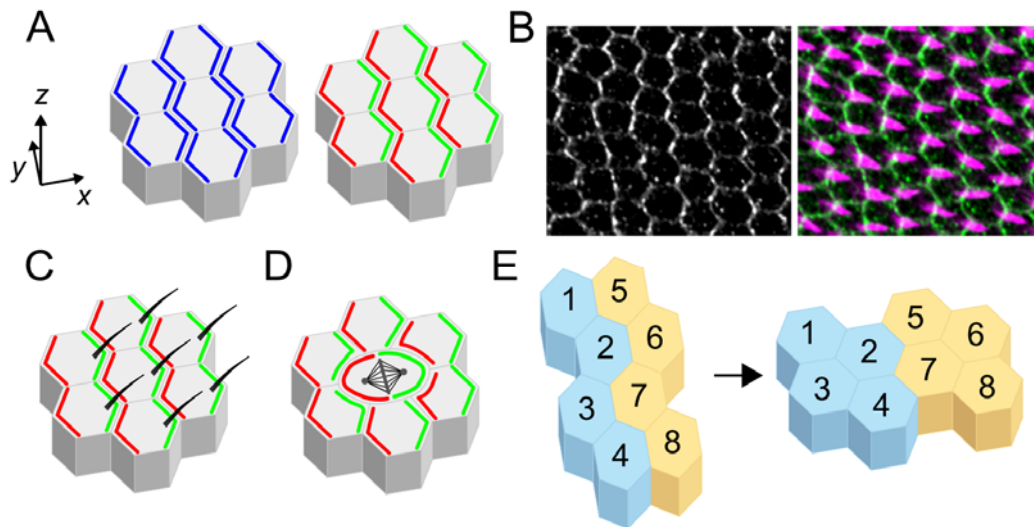
## 322 **Acknowledgements**

323

324 This work was supported by The Wellcome Trust (grant number 100986) and The  
325 University of Sheffield.

326  
327

**Figure 1**

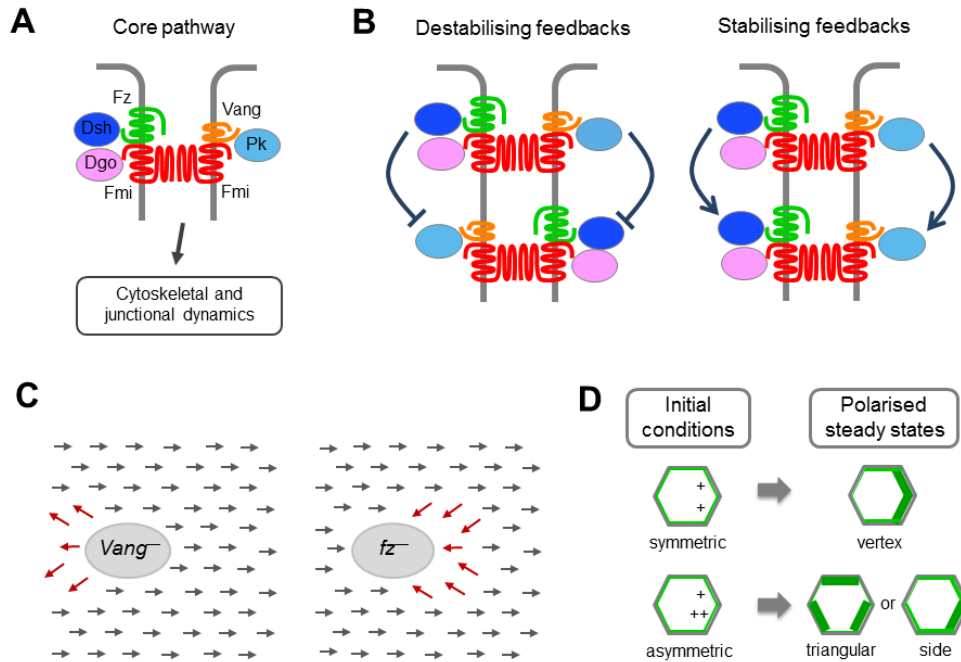


328  
329

330 **Planar polarity in epithelial morphogenesis.** (A) In addition to polarising along an  
331 apicobasal axis ( $z$ ), epithelial cells often exhibit planar polarity (also known as planar  
332 cell polarity) within the plane of the tissue ( $x, y$ ). Planar polarity arises from the non-  
333 uniform distribution of polarity proteins, which may exhibit axial (enriched on opposite  
334 sides of each cell; blue) or vectorial (enriched on one side; red and green) polarity.  
335 (B) Wild-type *Drosophila* pupal wing (28h after puparium formation) stained for Vang  
336 (grey and green), which has vectorial polarity, and trichomes (magenta) (C, D, E)  
337 Planar polarity coordinates the alignment and organisation of cellular and  
338 multicellular structures. These include: the formation of hairs and bristles, such as  
339 the trichomes produced on the distal side of each cell on the adult *Drosophila* wing  
340 surface (C); oriented divisions, as observed for example in cells in *Drosophila*  
341 imaginal discs (D); and (E) polarised cell movements and rearrangements, such as  
342 during convergent extension.

343 **Figure 2**

344



345

346

347

348

349

350

351

352

353

354

355

356

357

358

359

360

361

362

363

364

365

366

**Figure 2. Computational modelling of the core pathway in *Drosophila* wing**

**development.** (A) Intercellular core protein complex arrangement at the adherens

junction zone of *Drosophila* epithelial cells. The formation of an asymmetric

intercellular complex involves the transmembrane proteins Frizzled (Fz; green) and

Flamingo (Fmi; red) and the cytosolic proteins Dishevelled (Dsh; dark blue) and

Diego (Dgo; pink) at the distal end of one cell, and the transmembrane proteins Vang

Gogh (Vang; orange) and Fmi and the cytosolic protein Prickle (Pk; pale blue) at the

proximal end of the adjacent cell. Polarised localisation of complex components

leads to altered cytoskeletal and junctional dynamics, and thus altered cell

mechanics. (B) Possible feedback interactions between non-transmembrane factors

that, either alone or in combinations, could underlie amplification of asymmetry. For

example, Dsh may inhibit Pk binding to Vang. (C) Schematic of non-autonomous

phenotypes, observed in the *Drosophila* wing, around clones of cells mutant for Fz or

Vang. (D) Schematic of 2D simulation results from Fischer et al [23], showing that the

model of Amonlirdviman et al [22] does not give stable vertex polarised steady states

in the absence of a persistent global bias. A uniform array of hexagonal cells is

considered. In the upper panel, initial conditions are such that Fz is localised in all

compartments of each hexagonal cell with a small initial bias (+) in the two distal

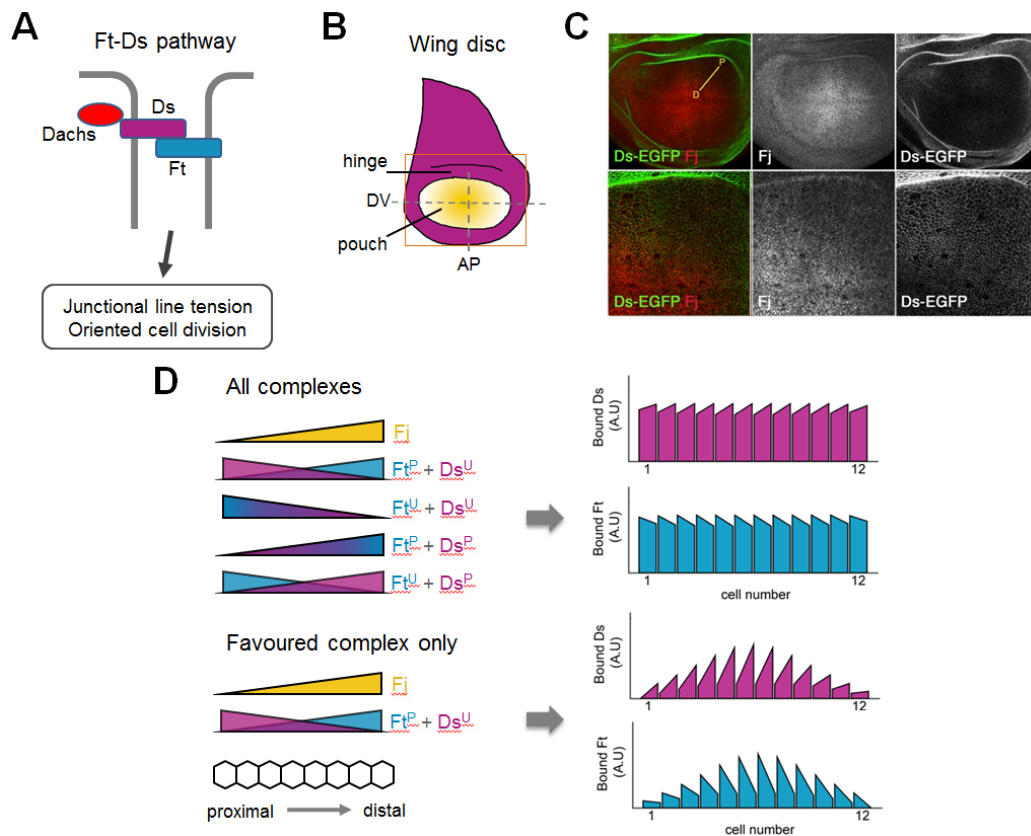
compartments. This initial bias is amplified by the feedbacks, while symmetry is

maintained, resulting in a final vertex polarity (thicker green edges). In the lower

367 panel, an initial bias is applied but with a small difference (either + or ++) between  
368 the two distal compartments. Again the initial bias is amplified, but given the noise in  
369 initial conditions, vertex polarity is not maintained.

370  
371

**Figure 3**



372  
373

374

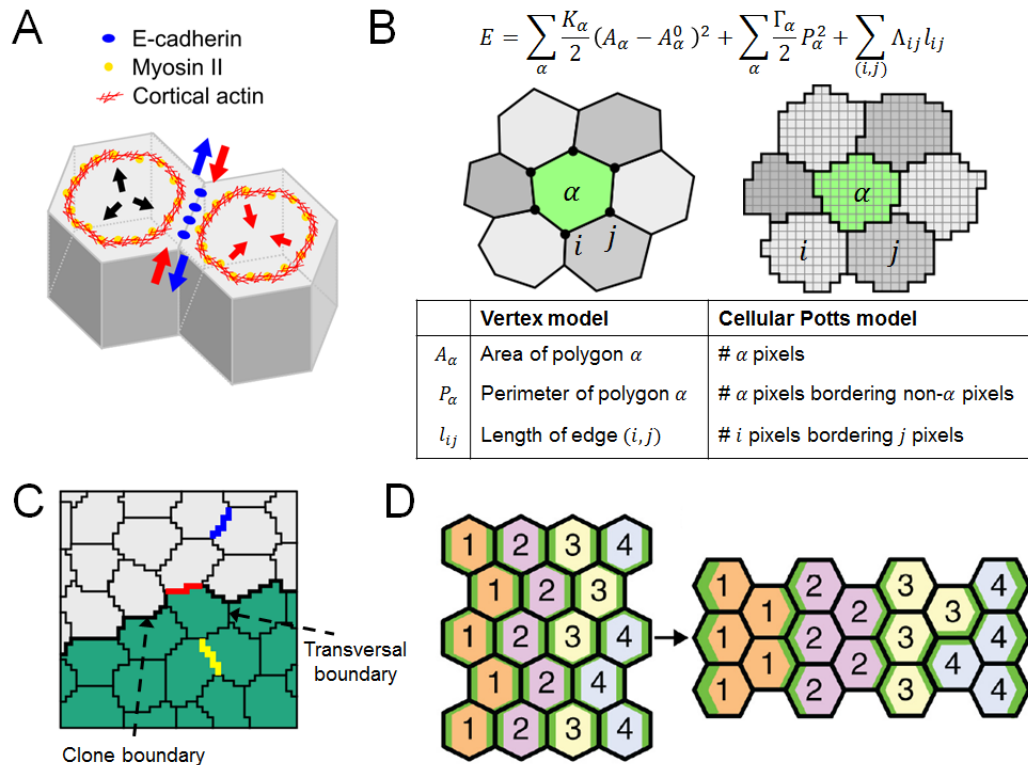
**Figure 3. Computational modelling of Ft-Ds pathway establishment in the**

375 ***Drosophila* wing.** (A) Fat (Ft; turquoise) and Dachshous (Ds; purple) bind  
376 heterophilically to form asymmetric intercellular complexes. Dachs (red), an atypical  
377 myosin, is recruited to colocalise with Ds, where it modulates junctional tension and  
378 orients cell division. (B) Cartoon of *Drosophila* 3<sup>rd</sup> instar larval wing disc. Ds (purple)  
379 is expressed at high levels in the hinge region, whereas Four-jointed (Fj; yellow) is  
380 expressed in a graded pattern in the pouch, which will go on to form the blade of the  
381 adult wing. Dorsoventral (DV) and anterioposterior (AP) compartment boundaries are  
382 shown by dashed lines. Orange box represents the cropped region shown in the  
383 upper panels of C. (C) Anti-Fj staining (red) of a wing disc expressing Ds-EGFP  
384 (green) as shown in Hale et al [42]. Fj is clearly graded along the proximodistal (PD)  
385 axis. (D) Simulation results based on the computational model of Hale et al [42].  
386 Graded Fj leads to opposing gradients of phosphorylated Ft/Ds (Ft<sup>P</sup>, Ds<sup>P</sup>) and  
387 unphosphorylated Ft/Ds (Ft<sup>U</sup>, Ds<sup>U</sup>). Upper panel - all four possible heterophilic  
388 complexes form, listed in order of preferential binding (i.e. the top complex is the  
389 most favoured), leading to cellular asymmetry of bound Ft and Ds complexes that are  
390 largely uniform across the tissue. Lower panel - only the most favoured complex

391 forms ( $Ft^P$  binding  $Ds^U$ ), thus polarisation and bound protein levels are much stronger  
392 in the middle of the tissue compared to the proximal and distal edges. Graphs show  
393 simulation results where each bar represents a cell, showing the relative amount of  
394 bound protein on the left and right sides in arbitrary units (A.U.).

395  
396

**Figure 4**



397  
398  
399

**Figure 4. Computational modelling of the mechanics of planar polarised**

400

**epithelia. (A)** Schematic of the forces arising from apically localised adhesion

401

molecules and cytoskeletal components in neighbouring epithelial cells. E-cadherin

402

binding between tends to reduce surface tension and expand cell-cell junctions (blue

403

arrows), while actomyosin imposes contractile forces at junctions and cell cortices

404

(red arrows), the latter counteracted by intracellular osmotic pressure (black arrows).

405

Each of these effector proteins can be regulated by upstream planar polarity signals.

406

**(B)** Comparison of the vertex and cellular Potts models of epithelial dynamics. Either

407

a force balance equation for each vertex (left) or Monte Carlo simulation and

408

exchange of pixels (right) is used to drive the tissue toward a configuration of

409

minimum 'energy',  $E$ . **(C)** Cellular Potts model of somatic clone rounding in

410

*Drosophila* pupal dorsal thorax [34]. Observed cell behaviours in Ft or Ds mutant

411

clones are recapitulated by assuming that Dachs polarisation results in line tensions

412

( $\Lambda_{ij}$ ) taking a high value for cell-cell junctions at a clone boundary (red), an

413

intermediate value for cell-cell junctions outside the clone (blue), and a low value for

414

cell-cell junctions within the clone (yellow). **(D)** Vertex model of active cell

415

intercalation during *Drosophila* germ-band extension [63]. Cell rearrangement results

416

in stripes of cells of the same identity becoming adjacent. Myosin II is enriched

417 preferentially at interfaces shared between cells of different identity (green).  
418 Convergent extension can be recapitulated by assuming that line tensions at cell-cell  
419 junctions ( $\Lambda_{ij}$ ) are increased by Myosin II enrichment and depend nonlinearly on the  
420 total length of contiguous interfaces a given cell has with cells of different identities,  
421 the latter assumption approximating the presence of actomyosin cables.



422 **References**

423

- 424 1. Green JB, Sharpe J: **Positional information and reaction-diffusion: two big**  
425 **ideas in developmental biology combine.** *Development* 2015, **142**:1203-1211.
- 426 2. LeGoff L, Lecuit T: **Mechanical Forces and Growth in Animal Tissues.** *Cold*  
427 *Spring Harb Perspect Biol* 2015, **8**:a019232.
- 428 3. Eder D, Aegerter C, Basler K: **Forces controlling organ growth and size.** *Mech*  
429 *Dev* 2017, **144**:53-61.
- 430 4. Julicher F, Eaton S: **Emergence of tissue shape changes from collective cell**  
431 **behaviours.** *Semin Cell Dev Biol* 2017.
- 432 5. Thompson BJ: **Cell polarity: models and mechanisms from yeast, worms and**  
433 **flies.** *Development* 2013, **140**:13-21.
- 434 6. Goodrich LV, Strutt D: **Principles of planar polarity in animal development.**  
435 *Development* 2011, **138**:1877-1892.
- 436 7. Hale R, Strutt D: **Conservation of Planar Polarity Pathway Function Across**  
437 **the Animal Kingdom.** *Annu Rev Genet* 2015, **49**:529-551.
- 438 8. Burak Y, Shraiman BI: **Order and stochastic dynamics in Drosophila planar**  
439 **cell polarity.** *PLoS Comput Biol* 2009, **5**:e1000628.
- 440 9. Ma D, Yang CH, McNeill H, Simon MA, Axelrod JD: **Fidelity in planar cell**  
441 **polarity signalling.** *Nature* 2003, **421**:543-547.
- 442 10. Butler MT, Wallingford JB: **Planar cell polarity in development and disease.**  
443 *Nat Rev Mol Cell Biol* 2017.
- 444 11. Aw WY, Devenport D: **Planar cell polarity: global inputs establishing cellular**  
445 **asymmetry.** *Curr Opin Cell Biol* 2017, **44**:110-116.
- 446 12. Bayly R, Axelrod JD: **Pointing in the right direction: new developments in the**  
447 **field of planar cell polarity.** *Nat Rev Genet* 2011, **12**:385-391.
- 448 13. Heller E, Fuchs E: **Tissue patterning and cellular mechanics.** *J Cell Biol* 2015,  
449 **211**:219-231.
- 450 14. Morelli LG, Uriu K, Ares S, Oates AC: **Computational approaches to**  
451 **developmental patterning.** *Science* 2012, **336**:187-191.
- 452 15. Strutt H, Strutt D: **Asymmetric localisation of planar polarity proteins:**  
453 **Mechanisms and consequences.** *Semin Cell Dev Biol* 2009, **20**:957-963.
- 454 16. Vinson CR, Adler PN: **Directional non-cell autonomy and the transmission of**  
455 **polarity information by the frizzled gene of Drosophila.** *Nature* 1987,  
456 **329**:549-551.
- 457 17. Taylor J, Abramova N, Charlton J, Adler PN: **Van Gogh: a new Drosophila**  
458 **tissue polarity gene.** *Genetics* 1998, **150**:199-210.

- 459 18. Strutt D, Strutt H: **Differential activities of the core planar polarity proteins**  
460 **during Drosophila wing patterning.** *Dev Biol* 2007, **302**:181-194.
- 461 19. Tree DR, Shulman JM, Rousset R, Scott MP, Gubb D, Axelrod JD: **Prickle**  
462 **mediates feedback amplification to generate asymmetric planar cell**  
463 **polarity signaling.** *Cell* 2002, **109**:371-381.
- 464 20. Jenny A, Reynolds-Kenneally J, Das G, Burnett M, Mlodzik M: **Diego and**  
465 **Prickle regulate Frizzled planar cell polarity signalling by competing for**  
466 **Dishevelled binding.** *Nat Cell Biol* 2005, **7**:691-697.
- 467 21. Axelrod JD, Tomlin CJ: **Modeling the control of planar cell polarity.** *Wiley*  
468 *Interdiscip Rev Syst Biol Med* 2011, **3**:588-605.
- 469 22. Amonlirdviman K, Khare NA, Tree DR, Chen WS, Axelrod JD, Tomlin CJ:  
470 **Mathematical modeling of planar cell polarity to understand domineering**  
471 **nonautonomy.** *Science* 2005, **307**:423-426.
- 472 23. Fischer S, Houston P, Monk NA, Owen MR: **Is a persistent global bias**  
473 **necessary for the establishment of planar cell polarity?** *PLoS One* 2013,  
474 **8**:e60064.
- 475 24. Le Garrec JF, Lopez P, Kerszberg M: **Establishment and maintenance of**  
476 **planar epithelial cell polarity by asymmetric cadherin bridges: a computer**  
477 **model.** *Dev Dyn* 2006, **235**:235-246.
- 478 25. Hazelwood LD, Hancock JM: **Functional modelling of planar cell polarity: an**  
479 **approach for identifying molecular function.** *BMC Dev Biol* 2013, **13**:20.
- 480 26. Abley K, De Reuille PB, Strutt D, Bangham A, Prusinkiewicz P, Maree AF,  
481 Grieneisen VA, Coen E: **An intracellular partitioning-based framework for**  
482 **tissue cell polarity in plants and animals.** *Development* 2013, **140**:2061-2074.
- 483 27. Schamberg S, Houston P, Monk NA, Owen MR: **Modelling and analysis of**  
484 **planar cell polarity.** *Bull Math Biol* 2010, **72**:645-680.
- 485 28. Ma D, Amonlirdviman K, Raffard RL, Abate A, Tomlin CJ, Axelrod JD: **Cell**  
486 **packing influences planar cell polarity signaling.** *Proc Natl Acad Sci U S A*  
487 2008, **105**:18800-18805.
- 488 29. Shimada Y, Yonemura S, Ohkura H, Strutt D, Uemura T: **Polarized transport of**  
489 **Frizzled along the planar microtubule arrays in Drosophila wing epithelium.**  
490 *Dev Cell* 2006, **10**:209-222.
- 491 30. Matis M, Russler-Germain DA, Hu Q, Tomlin CJ, Axelrod JD: **Microtubules**  
492 **provide directional information for core PCP function.** *Elife* 2014, **3**:e02893.
- 493 31. Thomas C, Strutt D: **The roles of the cadherins Fat and Dachous in planar**  
494 **polarity specification in Drosophila.** *Dev Dyn* 2012, **241**:27-39.

- 495 32. Simon MA, Xu A, Ishikawa HO, Irvine KD: **Modulation of fat:dachsous binding**  
496 **by the cadherin domain kinase four-jointed.** *Curr Biol* 2010, **20**:811-817.
- 497 33. Brittle AL, Repiso A, Casal J, Lawrence PA, Strutt D: **Four-jointed modulates**  
498 **growth and planar polarity by reducing the affinity of dachsous for fat.** *Curr*  
499 *Biol* 2010, **20**:803-810.
- 500 34. Bosveld F, Bonnet I, Guirao B, Tlili S, Wang Z, Petitalot A, Marchand R, Bardet  
501 PL, Marcq P, Graner F, et al.: **Mechanical control of morphogenesis by**  
502 **Fat/Dachsous/Four-jointed planar cell polarity pathway.** *Science* 2012,  
503 **336**:724-727.
- 504 35. Ambegaonkar AA, Pan G, Mani M, Feng Y, Irvine KD: **Propagation of**  
505 **Dachsous-Fat planar cell polarity.** *Curr Biol* 2012, **22**:1302-1308.
- 506 36. Willecke M, Hamaratoglu F, Sansores-Garcia L, Tao C, Halder G: **Boundaries of**  
507 **Dachsous Cadherin activity modulate the Hippo signaling pathway to**  
508 **induce cell proliferation.** *Proc Natl Acad Sci U S A* 2008, **105**:14897-14902.
- 509 37. Mao Y, Tournier AL, Bates PA, Gale JE, Tapon N, Thompson BJ: **Planar**  
510 **polarization of the atypical myosin Dachs orientes cell divisions in**  
511 **Drosophila.** *Genes Dev* 2011, **25**:131-136.
- 512 38. Bosveld F, Guirao B, Wang Z, Riviere M, Bonnet I, Graner F, Bellaiche Y:  
513 **Modulation of junction tension by tumor suppressors and proto-oncogenes**  
514 **regulates cell-cell contacts.** *Development* 2016, **143**:623-634.
- 515 39. Merkel M, Sagner A, Gruber FS, Etournay R, Blasse C, Myers E, Eaton S,  
516 Julicher F: **The balance of prickle/spiny-legs isoforms controls the amount**  
517 **of coupling between core and fat PCP systems.** *Curr Biol* 2014, **24**:2111-  
518 2123.
- 519 40. Mani M, Goyal S, Irvine KD, Shraiman BI: **Collective polarization model for**  
520 **gradient sensing via Dachsous-Fat intercellular signaling.** *Proc Natl Acad*  
521 *Sci U S A* 2013, **110**:20420-20425.
- 522 41. Jolly MK, Rizvi MS, Kumar A, Sinha P: **Mathematical modeling of sub-cellular**  
523 **asymmetry of fat-dachsous heterodimer for generation of planar cell**  
524 **polarity.** *PLoS One* 2014, **9**:e97641.
- 525 42. Hale R, Brittle AL, Fisher KH, Monk NA, Strutt D: **Cellular interpretation of the**  
526 **long-range gradient of Four-jointed activity in the Drosophila wing.** *Elife*  
527 2015, **4**.
- 528 43. Irvine KD, Wieschaus E: **Cell intercalation during Drosophila germband**  
529 **extension and its regulation by pair-rule segmentation genes.** *Development*  
530 1994, **120**:827-841.

- 531 44. Blankenship JT, Backovic ST, Sanny JS, Weitz O, Zallen JA: **Multicellular**  
532 **rosette formation links planar cell polarity to tissue morphogenesis.** *Dev*  
533 *Cell* 2006, **11**:459-470.
- 534 45. Zallen JA, Wieschaus E: **Patterned gene expression directs bipolar planar**  
535 **polarity in *Drosophila*.** *Dev Cell* 2004, **6**:343-355.
- 536 46. da Silva SM, Vincent JP: **Oriented cell divisions in the extending germband**  
537 **of *Drosophila*.** *Development* 2007, **134**:3049-3054.
- 538 47. Butler LC, Blanchard GB, Kabla AJ, Lawrence NJ, Welchman DP, Mahadevan L,  
539 Adams RJ, Sanson B: **Cell shape changes indicate a role for extrinsic tensile**  
540 **forces in *Drosophila* germ-band extension.** *Nat Cell Biol* 2009, **11**:859-864.
- 541 48. Akam M: **The molecular basis for metameric pattern in the *Drosophila***  
542 **embryo.** *Development* 1987, **101**:1-22.
- 543 49. Jaeger J, Surkova S, Blagov M, Janssens H, Kosman D, Kozlov KN, Manu,  
544 Myasnikova E, Vanario-Alonso CE, Samsonova M, et al.: **Dynamic control of**  
545 **positional information in the early *Drosophila* embryo.** *Nature* 2004,  
546 **430**:368-371.
- 547 50. Verd B, Crombach A, Jaeger J: **Dynamic Maternal Gradients Control Timing**  
548 **and Shift-Rates for *Drosophila* Gap Gene Expression.** *PLoS Comput Biol*  
549 2017, **13**:e1005285.
- 550 51. Guillot C, Lecuit T: **Mechanics of epithelial tissue homeostasis and**  
551 **morphogenesis.** *Science* 2013, **340**:1185-1189.
- 552 52. Wallingford JB: **Planar cell polarity and the developmental control of cell**  
553 **behavior in vertebrate embryos.** *Annu Rev Cell Dev Biol* 2012, **28**:627-653.
- 554 53. Devenport D: **The cell biology of planar cell polarity.** *J Cell Biol* 2014,  
555 **207**:171-179.
- 556 54. Warrington SJ, Strutt H, Strutt D: **The Frizzled-dependent planar polarity**  
557 **pathway locally promotes E-cadherin turnover via recruitment of RhoGEF2.**  
558 *Development* 2013, **140**:1045-1054.
- 559 55. Classen AK, Anderson KI, Marois E, Eaton S: **Hexagonal packing of**  
560 ***Drosophila* wing epithelial cells by the planar cell polarity pathway.** *Dev Cell*  
561 2005, **9**:805-817.
- 562 56. Fletcher AG, Cooper F, Baker RE: **Mechanocellular models of epithelial**  
563 **morphogenesis.** *Philos Trans R Soc Lond B Biol Sci* 2017, **372**.
- 564 57. Fletcher AG, Osterfield M, Baker RE, Shvartsman SY: **Vertex models of**  
565 **epithelial morphogenesis.** *Biophys J* 2014, **106**:2291-2304.

- 566 58. Marée AF, Grieneisen VA, Hogeweg P: **The Cellular Potts Model and**  
567 **biophysical properties of cells, tissues and morphogenesis.** In *Single-cell-*  
568 *based models in biology and medicine.* Edited by: Springer; 2007:107-136.
- 569 59. Osborne JM, Fletcher AG, Pitt-Francis JM, Maini PK, Gavaghan DJ: **Comparing**  
570 **individual-based approaches to modelling the self-organization of**  
571 **multicellular tissues.** *PLoS Comput Biol* 2017, **13**:e1005387.
- 572 60. Salbreux G, Barthel LK, Raymond PA, Lubensky DK: **Coupling mechanical**  
573 **deformations and planar cell polarity to create regular patterns in the**  
574 **zebrafish retina.** *PLoS Comput Biol* 2012, **8**:e1002618.
- 575 61. Bertet C, Sulak L, Lecuit T: **Myosin-dependent junction remodelling controls**  
576 **planar cell intercalation and axis elongation.** *Nature* 2004, **429**:667-671.
- 577 62. Pare AC, Vichas A, Fincher CT, Mirman Z, Farrell DL, Mainieri A, Zallen JA: **A**  
578 **positional Toll receptor code directs convergent extension in Drosophila.**  
579 *Nature* 2014, **515**:523-527.
- 580 63. Tetley RJ, Blanchard GB, Fletcher AG, Adams RJ, Sanson B: **Unipolar**  
581 **distributions of junctional Myosin II identify cell stripe boundaries that**  
582 **drive cell intercalation throughout Drosophila axis extension.** *Elife* 2016, **5**.
- 583 64. Lan H, Wang Q, Fernandez-Gonzalez R, Feng JJ: **A biomechanical model for**  
584 **cell polarization and intercalation during Drosophila germband extension.**  
585 *Phys Biol* 2015, **12**:056011.
- 586 65. Aigouy B, Farhadifar R, Staple DB, Sagner A, Roper JC, Julicher F, Eaton S:  
587 **Cell flow reorients the axis of planar polarity in the wing epithelium of**  
588 **Drosophila.** *Cell* 2010, **142**:773-786.
- 589 66. Chien YH, Keller R, Kintner C, Shook DR: **Mechanical strain determines the**  
590 **axis of planar polarity in ciliated epithelia.** *Curr Biol* 2015, **25**:2774-2784.
- 591 67. Aw WY, Heck BW, Joyce B, Devenport D: **Transient Tissue-Scale Deformation**  
592 **Coordinates Alignment of Planar Cell Polarity Junctions in the Mammalian**  
593 **Skin.** *Curr Biol* 2016, **26**:2090-2100.
- 594 68. Bielmeier C, Alt S, Weichselberger V, La Fortezza M, Harz H, Julicher F,  
595 Salbreux G, Classen AK: **Interface Contractility between Differently Fated**  
596 **Cells Drives Cell Elimination and Cyst Formation.** *Curr Biol* 2016, **26**:563-  
597 574.
- 598 69. Ossipova O, Kim K, Lake BB, Itoh K, Ioannou A, Sokol SY: **Role of Rab11 in**  
599 **planar cell polarity and apical constriction during vertebrate neural tube**  
600 **closure.** *Nat Commun* 2014, **5**:3734.

- 601 70. Heller D, Hoppe A, Restrepo S, Gatti L, Tournier AL, Tapon N, Basler K, Mao Y:  
602 **EpiTools: An Open-Source Image Analysis Toolkit for Quantifying**  
603 **Epithelial Growth Dynamics.** *Dev Cell* 2016, **36**:103-116.
- 604 71. Farrell DL, Weitz O, Magnasco MO, Zallen JA: **SEGGA: a toolset for rapid**  
605 **automated analysis of epithelial cell polarity and dynamics.** *Development*  
606 2017, **144**:1725-1734.
- 607 72. Etournay R, Merkel M, Popovic M, Brandl H, Dye NA, Aigouy B, Salbreux G,  
608 Eaton S, Julicher F: **TissueMiner: A multiscale analysis toolkit to quantify**  
609 **how cellular processes create tissue dynamics.** *Elife* 2016, **5**.
- 610 73. Sugimura K, Lenne PF, Graner F: **Measuring forces and stresses in situ in**  
611 **living tissues.** *Development* 2016, **143**:186-196.
- 612 74. Bambardekar K, Clement R, Blanc O, Chardes C, Lenne PF: **Direct laser**  
613 **manipulation reveals the mechanics of cell contacts in vivo.** *Proc Natl Acad*  
614 *Sci U S A* 2015, **112**:1416-1421.